UC Riverside
UC Riverside Previously Published Works

Title

Oxidation of Cr(III)–Fe(III) Mixed-Phase Hydroxides by Chlorine: Implications on the Control of Hexavalent Chromium in Drinking Water

Permalink

Journal

Environmental Science and Technology, 52(14)

ISSN

0013-936X

Authors

Chebeir, Michelle
Liu, Haizhou

Publication Date

2018-07-17

DOI

10.1021/acs.est.7b06013

Peer reviewed

Oxidation of Cr(III)−Fe(III) Mixed-Phase Hydroxides by Chlorine: Implications on the Control of Hexavalent Chromium in Drinking Water

Michelle Chebeir and Haizhou Liu*

Department of Chemical and Environmental Engineering, University of California at Riverside, Riverside, California 92521, United States

S *Supporting Information*

ABSTRACT: The occurrence of chromium (Cr) as an inorganic contaminant in drinking water is widely reported. One source of Cr is its accumulation in iron-containing corrosion scales of drinking water distribution systems as Cr(III)−Fe(III) hydroxide, that is, $Fe_xCr_{(1-x)}(OH)_{3(s)}$, where x represents the Fe(III) molar content and typically varies between 0.25 and 0.75. This study investigated the kinetics of inadvertent hexavalent chromium Cr(VI) formation via the oxidation of $Fe_xCr_{(1-x)}(OH)_{3(s)}$ by chlorine as a residual disinfectant in drinking water, and examined the impacts of Fe(III) content and drinking water chemical parameters including pH, bromide and bicarbonate on the rate of Cr(VI) formation. Data showed that an increase in Fe(III) molar content resulted in a significant decrease in the stoichiometric Cr(VI) yield and the rate of Cr(VI) formation, mainly due to chlorine decay induced by Fe(III) surface sites. An increase in bicarbonate enhanced the rate of Cr(VI) formation, likely due to the formation of Fe(III)-carbonato surface complexes that slowed down the scavenging reaction with chlorine. The presence of bromide significantly accelerated the oxidation of $Fe_xCr_{(1-x)}(OH)_{3(s)}$ by chlorine, resulting from the catalytic effect of bromide acting as an electron shuttle. A higher solution pH between 6 and 8.5 slowed down the oxidation of Cr(III) by chlorine. These findings suggested that the oxidative conversion of chromium-containing iron corrosion products in drinking water distribution systems can lead to the occurrence of Cr(VI) at the tap, and the abundance of iron, and a careful control of pH, bicarbonate and bromide levels can assist the control of Cr(VI) formation.

INTRODUCTION

Chromium (Cr) can exist as hexavalent Cr(VI) and trivalent Cr(III) in drinking water. Cr(VI) is highly mobile and toxic, whereas Cr(III) forms minerals with low solubility at circumneutral pH and is also considered a micronutrient.[1,2] The State of California set a new drinking water regulation specifically for Cr(VI) at 10 μg/L in 2014.[3] The U.S. EPA regulates total chromium in drinking water at 100 μg/L, and a federal regulation solely for Cr(VI) may be established in the future.[4] Traditional anthropogenic sources typically come from industrial waste discharge.[5−7] In addition, natural occurrence of Cr(VI) originates from the natural weathering of Cr(III)-containing aquifer minerals in groundwater.[8−10]

In recent years, in situ generation of Cr(VI) in drinking water distribution systems from Cr-containing corrosion scales has drawn an increasing attention.[11,12] Corrosion products in drinking water pipes are found to contain up to 0.5% chromium by weight, far exceeding its natural abundance in the earth crust.[13−15] In particular, considering that nearly 70% of pipes in water distribution systems in the U.S. are composed of iron materials (e.g., cast iron, ductile iron and cement-lined iron), chromium can accumulate extensively in iron corrosion scales over time.[16−20] Chromium is typically present at trace levels below regulatory standards in treated drinking water, but over decades it can accumulate to very

high levels in the corroded solids in distribution systems. In addition, iron piping materials are found to contain chromium impurities that serve as in situ sources.[21−23] When coexisting with iron, Cr(III) forms mixed phases of Cr(III)−Fe(III) hydroxide, that is, $Fe_xCr_{(1-x)}(OH)_{3(s)}$, where x represents the Fe(III) molar content and typically varies between 0.25 and 0.75.[24−26] In addition, $Fe_xCr_{(1-x)}(OH)_{3(s)}$ widely exists in iron-rich aquifer materials and its oxidation by Mn(IV) oxides contributes to the natural occurrence of Cr(VI) in ground-water.[27−29]

The occurrence of Cr(VI) in drinking water distribution systems depends on a cascade of redox processes. In particular, the oxidation of Cr(III) solids by the residual disinfectant chlorine can take place in distribution systems, and results in the risk of an inadvertent generation of Cr(VI) at the tap. Nationwide surveys have indicated that the reaction pathways depended on Cr(III) speciation and its redox reactivity in distribution systems.[11,17,30] Field sampling data from the third round of U.S. Environmental Protection Agency Unregulated Contaminant Monitoring Rule

Table 1. Characteristics of Synthesized Cr(III)−Fe(III) Hydroxide $Fe_xCr_{(1-x)}(OH)_{3(s)}$

Cr(III)−Fe(III) hydroxide chemical formula	BET surface area (m²/g)	pH_{pzc}	$\log K_{sp}{}^a$	$E°$ (V)[b]
$Fe_{0.25}Cr_{0.75}(OH)_{3(s)} \cdot 1.5H_2O$	279	5.3	−33.8	0.23
$Fe_{0.5}Cr_{0.5}(OH)_{3(s)} \cdot H_2O$	355	3.8	−34.5	0.38
$Fe_{0.75}Cr_{0.25}(OH)_{3(s)} \cdot 1.5H_2O$	198	5.5	−34.7	0.82

[a] the value of K_{sp} is based on dissolution reactions listed in Text S1 in the SI. [b] $E°$ is the standard half-reaction redox potential of the redox couple between $Fe_xCr_{(1-x)}(OH)_{3(s)}$ and $CrO_4{}^{2-}$.

(UCMR3) indicated that Cr(VI) levels increased from the entry to exit point of many distribution systems nationwide, and this trend correlated with the presence of chlorine as the residual disinfectant.[11] Recent studies also showed that the oxidation of Cr(III) solids by chlorine can increase Cr(VI) levels in drinking water.[12,31,32] In addition, mixed phases of Cr(III) oxides with other metals, for example, $Cu_2Cr_2O_{5(s)}$, exhibit a higher redox reactivity than pure phases of Cr(III).[12] Similarly, the coexistence of Fe(III) in $Fe_xCr_{(1-x)}(OH)_{3(s)}$ can possess unique reactivity with chlorine to generate Cr(VI), and the aging of Cr(III) solids can also impact its redox reactivity; however, there is little knowledge on the formation of Cr(VI) from $Fe_xCr_{(1-x)}(OH)_{3(s)}$ in drinking water.

Furthermore, the impacts of water chemical parameters including pH, bromide and bicarbonate on the reactivity of Cr(III)−Fe(III) hydroxide remain unknown. Bicarbonate and pH are important parameters to control corrosion in distribution systems.[33,34] They impact complexation of metal surface carbonato and hydroxo species, and consequently surface redox reactivity of metal oxides.[35] pH can also impact the speciation of chlorine and its oxidative capacity. Bromide exhibits a catalytic effect on the chlorine-driven oxidation of transition metals.[36] Recent studies show that bromide level in drinking water can increase by as much as 20 times in the future due to seawater intrusion, desalination, water reuse and brine discharge from alternative energy production (e.g., shale gas).[37]

Considering the importance of understanding the reactivity of $Fe_xCr_{(1-x)}(OH)_{3(s)}$ and consequently the development of effective Cr(VI) control strategies in water distribution infrastructure, the objectives of this study were to investigate the mechanisms of Cr(VI) formation via $Fe_xCr_{(1-x)}(OH)_{3(s)}$ oxidation by chlorine, and to quantify the impacts of Fe(III), bicarbonate, pH and bromide on the reaction kinetics and stoichiometry.

■ MATERIALS AND METHODS

All chemicals used in this study were reagent grade or higher. All solutions were prepared using deionized (DI) water (resistivity >18.2 MΩ, Millipore System). Cr(III)−Fe(III) hydroxide solids with three different Fe(III) molar contents were synthesized using a standard protocol.[38] In brief, solutions of $Fe(NO_3)_3$ and $CrCl_3$ were mixed at a molar ratio of either 0.3:1, 1:1, or 3:1 at pH 7 for 3 days. Ferrihydrite $Fe(OH)_{3(s)}$ was synthesized via the hydrolysis of $Fe(NO_3)_3$ at pH 7.[39] All solids were washed with DI water three times and then centrifuged, frozen overnight and lyophilized for 24 h. The freeze-dried solids were sequentially sieved through NO. 50, 170, and 325 mesh sieves. Sieved particles with nominal sizes between 45 and 90 μm were collected and used in this study. Because of the amorphous
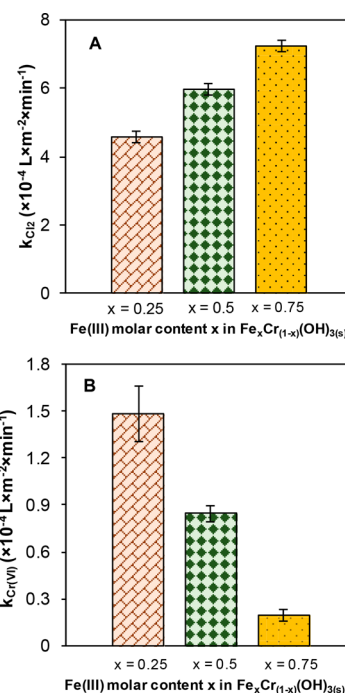
Figure 1. (A) Chlorine consumption and (B) Cr(VI) formation rate constants during the oxidation of iron chromite by chlorine. [Cr(III)] = 2.8 mM, [HOCl] = 20 mg Cl_2/L, [Cr(III)]:[Cl_2] = 10:1, ionic strength = 10 mM, pH 7.0.

nature of $Fe_xCr_{(1-x)}(OH)_{3(s)}$ solids, X-ray diffraction (XRD) was not capable of characterizing their chemical compositions. To confirm the chemical compositions of synthesized solids, particles were acid digested, and Cr and Fe percentages were analyzed with an Agilent 7700 inductively coupled plasma-mass spectrometry. The BET surface area of solids was measured using a Micromeritics ASAP 2020 surface area analyzer. Zeta potentials of $Fe_xCr_{(1-x)}(OH)_{3(s)}$ were measured by a Zeta Potential Analyzer (Brookhaven Instruments). The physicochemical parameters of the synthesized solids are listed in Table 1.

A 28 mM free chlorine stock solution diluted from a NaOCl solution (Sigma-Aldrich) was freshly prepared every week. The concentration of chlorine was verified by titration with potassium permanganate.[40] Before the start of an experiment, all solutions were purged with N_2 gas to remove the dissolved O_2. Following that, 0.28 mM of chlorine (i.e., 20 mg Cl_2/L) was quickly added into the reactor tube and mixed with $Fe_xCr_{(1-x)}(OH)_{3(s)}$. This chlorine concentration was higher than typical drinking water residual disinfectant concentration, but provided useful insight into reaction kinetics. The dosages of different Cr(III)−Fe(III) hydroxide solids were controlled so that the Cr(III) molar concentration was constant at 2.8 mM, corresponding to a Cr(III)-to-chlorine ratio of 10:1. In some experiments, ferrihydrite was used to examine the effect of Fe(III).

The solution pH was maintained at a targeted value (±0.2 pH units) between 6.0 and 8.5 with 10 mM phosphate buffer. Control experiments confirmed that the presence of phosphate buffer had a negligible impact on the reaction kinetics. Bromide level was varied between 0.1 and 1 mg/L, and bicarbonate between 1 and 5 mM. In experiments with varying bicarbonate, 10 mM MOPS (3-morpholinopropane-1-sulfonic acid) was added as the pH buffer to avoid the
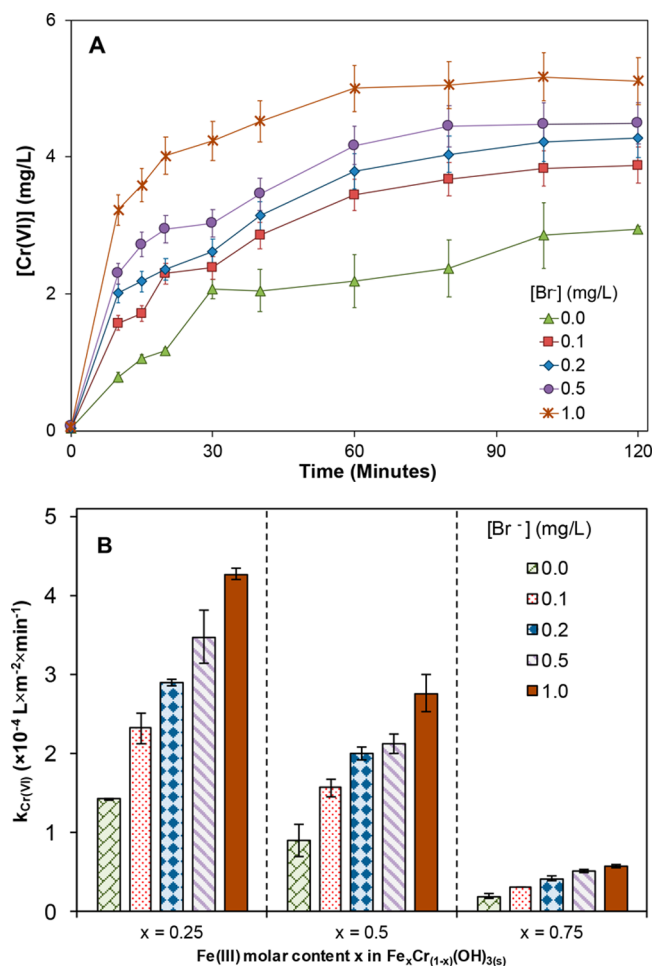
Figure 2. (A) Time profile for Cr(VI) generation from chlorine oxidation of $Fe_{0.5}Cr_{0.5}(OH)_{3(s)}$. (B) Effect of bromide on the surface area normalized second-order Cr(VI) formation rate constants of Cr(III)−Fe(III) hydroxide oxidation by chlorine. Initial $[Cr(III)] = 2.8$ mM, $[HOCl] = 20$ mg Cl_2/L, $Cr(III):Cl_2 = 10:1$, ionic strength $= 10$ mM, pH 7.

Figure 3. (A) Impact of carbonate concentration on chlorine consumption the oxidation of $Fe_{0.75}Cr_{0.25}(OH)_{3(s)}$ by chlorine. (B) Effect of carbonate on the surface area normalized second-order Cr(VI) formation rate constants of Cr(III)−Fe(III) hydroxide oxidation by chlorine. Initial $[Cr(III)] = 2.8$ mM, $[HOCl] = 20$ mg Cl_2/L, $Cr(III):Cl_2 = 10:1$, ionic strength $= 10$ mM, pH 7.

potential interference of phosphate on Fe(III) surface complexation.[41,42] The solution ionic strength was kept at 10 mM by adding a requisite amount of $NaClO_4$. In some experiments, an excess of 1 mM of benzoic acid (BA) was added as a chemical probe to assess the generation of reactive radical species during chlorine oxidation. All chlorine oxidation experiments were conducted in sealed glass tube reactors with no headspace or light exposure, and placed on a rotator to ensure continuous mixing. The ambient temperature was 20 °C ± 2 °C.

Sacrificial tubes were removed from the rotator at predetermined time intervals for chemical analyses. In some experiments, solutions were purged with N_2 gas for 20 min to minimize the presence of dissolved O_2, and the subsequent generation of dissolved O_2 from the reaction was measured using a Mettler-Toledo probe. The leakage of O_2 to the ambient environment was minimal. After that, concentrated NaOH was added to the suspension to release potentially adsorbed Cr(VI) from $Fe_xCr_{(1-x)}(OH)_{3(s)}$, followed by filtration of the suspension through a 0.22 μm Millipore PTFE filter. The concentration of Cr(VI) in the filtrate was measured using the diphenylcarbazide method.[40] Chlorine concentration was measured using a modified DPD method,

in which thioacetamide was added to eliminate any potential interference from Cr(VI).[12] Data modeling using the Goal Seek function with Microsoft Excel was applied to obtain the reaction kinetics rate constants, and to correlate the relationship between the stoichiometric ratios of chlorine consumption and Cr(VI) formation rates.

■ RESULTS AND DISCUSSION

Kinetics of Cr(III)−Fe(III) Hydroxide Oxidation by Chlorine and Cr(VI) Formation. The standard half-reaction redox potential of $Fe_xCr_{(1-x)}(OH)_{3(s)}$ solids are calculated in Supporting Information (SI) Text S1. The values indicate that the oxidation of $Fe_xCr_{(1-x)}(OH)_{3(s)}$ by chlorine is thermodynamically feasible. To examine the reaction kinetics, a second-order reaction kinetics model was introduced to quantify the rates of chlorine consumption and Cr(VI) formation:

$$\frac{d[Cl_2]}{dt} = -k_{Cl_2}[Cr(III)_s][Cl_2](S_{Cr(III)_{(s)}}) \quad (1)$$

$$\frac{d[Cr(VI)]}{dt} = k_{Cr(VI)}[Cr(III)_s][Cl_2](S_{Cr(III)_{(s)}}) \quad (2)$$

k_{Cl2} and $k_{Cr(VI)}$ are the surface-area normalized rate constants for chlorine consumption and Cr(VI) formation, respectively
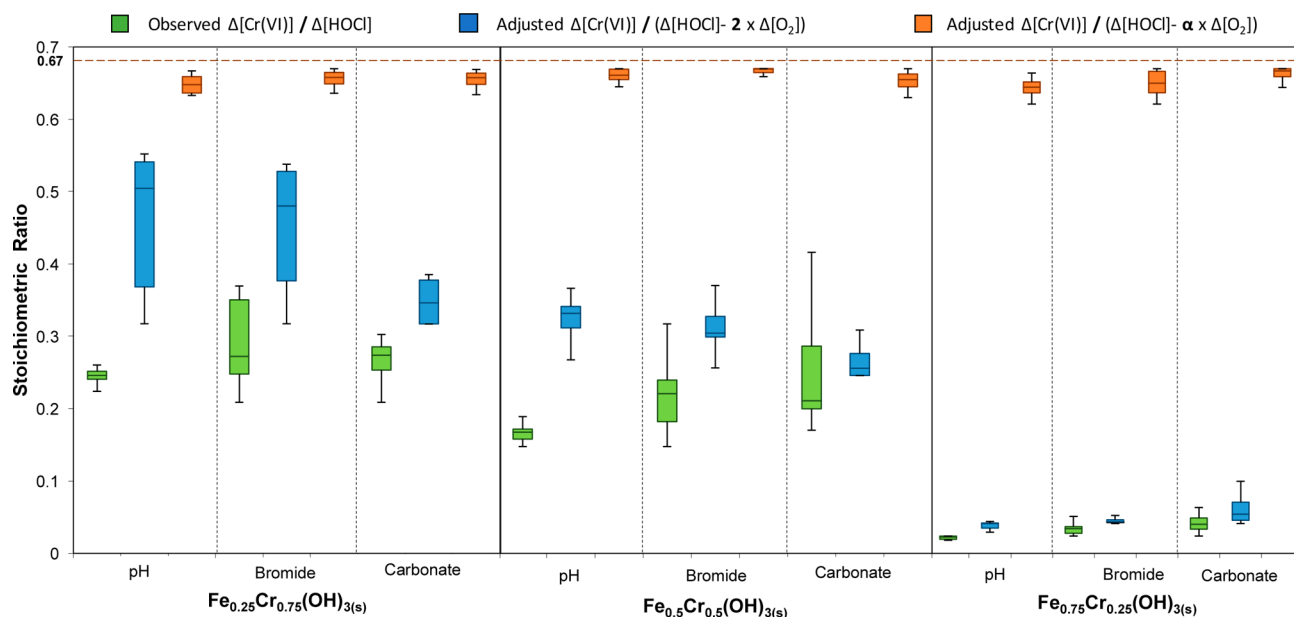
Figure 4. Average stoichiometric ratio for varying water quality parameters and different Cr(III)−Fe(III) hydroxides. The green box plots represent the stoichiometric ratio based on $\Delta Cr(VI)/\Delta HOCl$. The blue box plots represent the stoichiometric ratio based on $\Delta Cr(VI)/(\Delta HOCl - 2\Delta O_2)$. The orange box plots represent the stoichiometric ratio based on $\Delta Cr(VI)/(\Delta HOCl - \alpha\Delta O_2)$. The whiskers of the box plot represent the 10th and 90th percentiles of concentration. The lower quartile, middle and upper quartile represent the 25th, 50th, and 75th percentile values.

$(L \cdot m^{-2} \cdot min^{-1})$. $[Cl_2]$ is the free chlorine concentration (mol/L), $[Cr(III)_{(s)}]$ is the concentration of Cr(III) in Cr(III)−Fe(III) hydroxide (g/L), and $S_{Cr(III)(s)}$ is the BET surface area of Cr(III)−Fe(III) hydroxide (m^2/g). The model-fitted data correlated well with the experimental data, with a minimal R^2 ranging between 0.85 and 0.95 for every set of experiment.

Surface-area normalized rate constants of chlorine consumption with Cr(III)−Fe(III) hydroxide increased with Fe(III) molar contents, that is, the value of x in $Fe_xCr_{(1-x)}(OH)_{3(s)}$ (Figure 1A). These k_{Cl2} values were 2−3 times higher than the rate constants observed with pure phases of Cr(III) oxides that do not contain Fe(III), for example, $Cr(OH)_{3(s)}$ and $Cr_2O_{3(s)}$.[12] Meanwhile, the rate constant of Cr(VI) formation decreased significantly with increasing Fe(III) content: from 1.5×10^{-4} to 1.9×10^{-5} L·m^{-2}·min^{-1} when the value of x in $Fe_xCr_{(1-x)}(OH)_{3(s)}$ increased from 0.25 to 0.75 (Figure 1B). This trend suggested that the presence of Fe(III) in Cr(III)-containing solids preferentially promoted the reaction kinetics of chlorine consumption but diminishing Cr(VI) formation.

Bromide. The presence of bromide enhanced the reaction kinetics. As the bromide concentration increased from 0 to 1 mg/L, an enhanced Cr(VI) formation was observed (Figure 2A), and the rate constant of $k_{Cr(VI)}$ increased by approximately 3 times (Figure 2B). Meanwhile, chlorine consumption kinetics accelerated (SI Figure S1A) and the rate constant approximately doubled (SI Figure S1B). The promotive effects of bromide on the oxidation reaction resulted from an electron shuttle mechanism. Bromide readily reacted with HOCl to generate hypobromous acid (HOBr).[43] Prior studies demonstrated that HOBr is more electrophilic than HOCl and consequently exhibited a faster kinetics in oxidizing electron-rich compounds including transition metals and organics.[36,44,45] Control experiments with HOBr also showed that HOBr oxidized $Fe_xCr_{(1-x)}(OH)_{3(s)}$ much faster than HOCl did (SI Figure S2). Therefore, in a bromide-

containing system, HOBr becomes the primary oxidant as bromide essentially acts as an electron shuttle that drives the oxidation of Cr(III)−Fe(III) hydroxide to Cr(VI) by chlorine:

$$Fe_xCr_{(1-x)}(OH)_{3(s)} + HOCl \underset{HOBr}{\overset{Br^-}{\rightleftharpoons}} CrO_4^{2-} + Fe^{3+} + H^+ + Cl^- \quad (3)$$
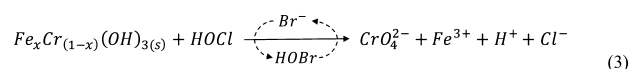
Bicarbonate. Bicarbonate exhibited a moderate impact on the reaction kinetics. With increasing total bicarbonate concentration $(TOTCO_3)$ from 0 to 5 mM at pH 7, the rate constant of Cr(VI) formation increased by approximately 200% (Figure 3A), and $Fe_xCr_{(1-x)}(OH)_{3(s)}$ with a lower Fe(III) molar content exhibited a higher sensitivity to the impact of bicarbonate on the rate of Cr(VI) formation (Figure 3B). Meanwhile, the rate of chlorine consumption increased by an average of 75% with the same amount of bicarbonate increase (SI Figure S3).

The impact of bicarbonate on the reaction kinetics is likely due to the formation of Fe(III)-carbonato complexes, which has been known to decrease the redox reactivity of Fe(III) surface sites.[35] In contrast, bicarbonate had a negligible effect on the redox reactivity of Cr(III) surface sites, as demonstrated by the negligible effect of bicarbonate on the oxidation of a pure phase of Cr(III) solid, that is, $Cr(OH)_{3(s)}$ by chlorine (SI Figure S4). Therefore, the presence of bicarbonate suppressed the reactivity of Fe(III) surface sites on $Fe_xCr_{(1-x)}(OH)_{3(s)}$ with respect to chlorine, and increased the availability of Cr(III) surface site subject to chlorine oxidation. As a result, the presence of bicarbonate enhanced the rate of Cr(VI) formation via $Fe_xCr_{(1-x)}(OH)_{3(s)}$ oxidation.

pH. The reaction kinetics were observed to decrease with increasing pH. The rate of chlorine consumption decreased by an average of 40% with pH rising from 6.0 to 8.5. For example, the chlorine consumption rate constant of $Fe_{0.75}Cr_{0.25}(OH)_{3(s)}$ declined from 9.2×10^{-4} to 5.3×10^{-4} L·m^{-2}·min^{-1} when pH increased from 6.0 to 8.5 (SI Figure S5A). The Cr(VI) formation rate constant from
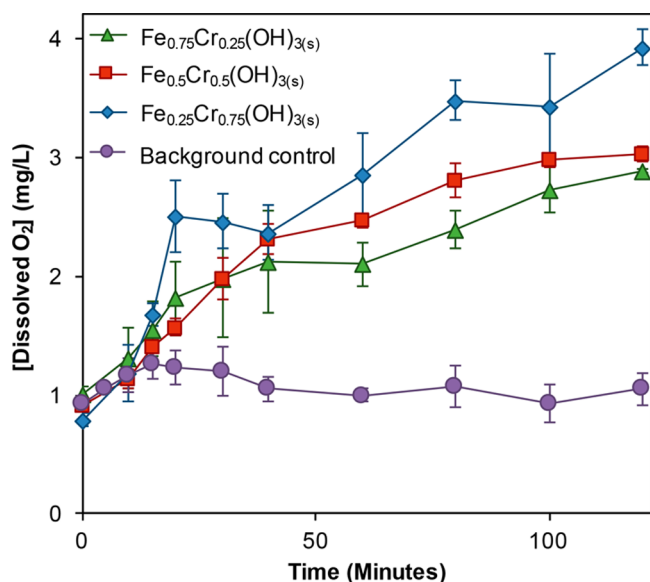
Figure 5. Oxygen generation over the course of the reaction. Initial [Cr(III)] = 2.8 mM, [HOCl] = 20 mg Cl$_2$/L, Cr(III):Cl$_2$ = 10:1, ionic strength = 10 mM, pH 7. Oxygen data in the background control represents the average background oxygen levels from control experiments that include only chlorine or Fe$_x$Cr$_{(1-x)}$(OH)$_{3(s)}$.

Fe$_{0.25}$Cr$_{0.75}$(OH)$_{3(s)}$ decreased from 2.4×10^{-5} to 8.0×10^{-6} L·m^{-2}·min^{-1} when pH increased from 6.0 to 8.5 (SI Figure S5B). The pH effect was likely associated with metal hydroxo complexation on the surface of Fe$_x$Cr$_{(1-x)}$(OH)$_{3(s)}$. For example, the solution pH affects Cr(III)-hydroxo surface complexation.[46,47] Measurement of zeta potential showed that the surface of Fe$_x$Cr$_{(1-x)}$(OH)$_{3(s)}$ became more negatively charged with increasing pH (SI Figure S6), suggesting that Cr(III) surface complexes with a higher extent of hydroxylation predominated at higher pHs and they had a lower redox reactivity with chlorine. In addition, at higher pHs, especially above its pK value at 7.6, chlorine speciation favors the deprotonated form of OCl$^-$. The protonated HOCl is a more facile oxidant than the deprotonated OCl$^-$,[48] therefore, an increase in pH from 6 to 8.5 also converts chlorine to a less effective oxidant and contributes to the slow-down of Fe$_x$Cr$_{(1-x)}$(OH)$_{3(s)}$ oxidation.

Reaction Stoichiometry and Cr(VI) Formation Mechanisms. The theoretical stoichiometry of the reaction, defined as the molar ratio of Cr(VI) generated to chlorine consumed, that is, $\Delta[Cr(VI)]/\Delta[HOCl]$, is 0.67 based on the number of electron transfer in the redox reaction. Experimental data with Fe$_x$Cr$_{(1-x)}$(OH)$_{3(s)}$ showed that the observed stoichiometry of ΔCr(VI)/ΔHOCl was between 0.02 and 0.24 for all three Fe$_x$Cr$_{(1-x)}$(OH)$_{3(s)}$ solids under different chemical conditions (green-color box plots in Figure 4). The under-stoichiometric formation of Cr(VI) was likely associated with additional reaction pathways. First, the oxidation of Cr(III) can generate Cr(V) oxide intermediates.[12] Autodecomposition of Cr(V) intermediates reproduces Cr(III) and dissolved O$_2$, resulting in one molecule of O$_2$ generation for every two molecules of chlorine consumption. Indeed, a significant amount of dissolved O$_2$ formation was observed during the oxidation of Cr(III)−Fe(III) hydroxide (Figure 5). To take this reaction pathway into consideration, an adjusted stoichiometric ratio was calculated as $\Delta[Cr(VI)]/(\Delta[HOCl] - 2 \times \Delta[O_2])$. The adjusted stoichiometry increased significantly, but still fell
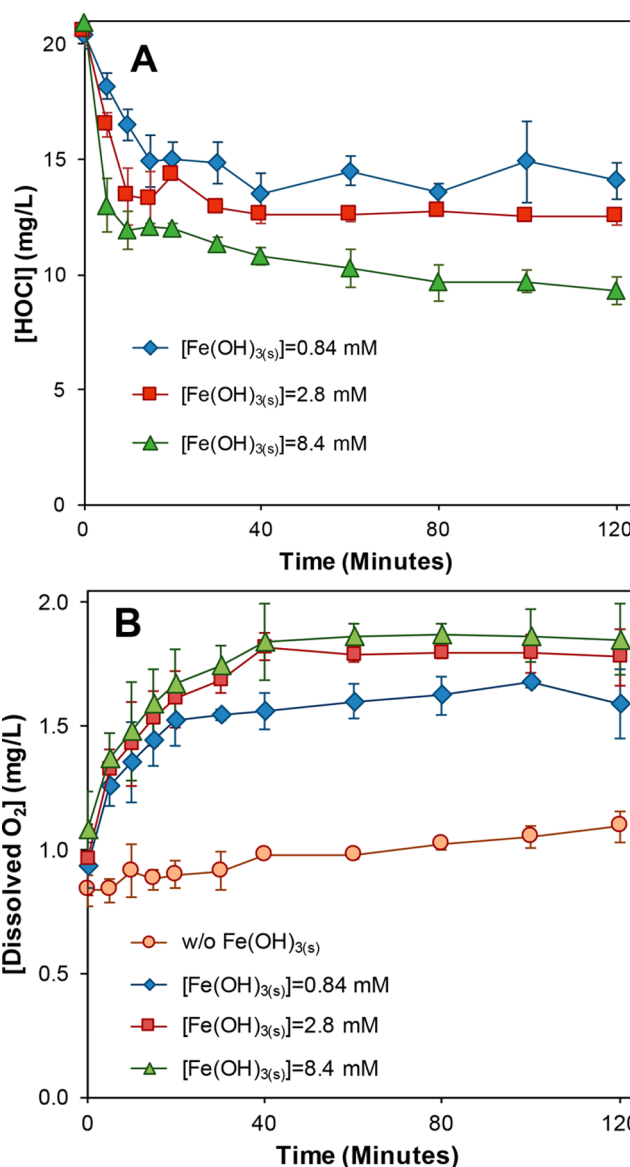
Figure 6. (A) Chlorine decrease in the presence of ferrihydrite. (B) Oxygen generation in the presence of ferrihydrite. Average background oxygen is 1 mg/L. Initial [HOCl] = 20 mg Cl$_2$/L, ionic strength = 10 mM, pH 7.0.

below the theoretical value of 0.67 (blue-color box plots in Figure 4). Second, as the x value in Fe$_x$Cr$_{(1-x)}$(OH)$_{3(s)}$ increased from 0.25 to 0.75, the stoichiometry of $\Delta[Cr(VI)]/\Delta[HOCl]$ decreased significantly (green- and blue-color box plots in Figure 4), accompanied by a 36% increase in oxygen generation (Figure 5). This suggested an additional reaction pathway specific to the presence of Fe(III) in Fe$_x$Cr$_{(1-x)}$(OH)$_{3(s)}$ that consumed chlorine without Cr(VI) generation.

To further investigate the reaction mechanism involving Fe(III) surface sites, additional control experiments were conducted in the presence of a pure phase of Fe(III) solid, that is, ferrihydrite Fe(OH)$_{3(s)}$. Data showed that the chlorine decay was accelerated with the introduction of ferrihydrite (Figure 6A), and was accompanied by the generation of dissolved O$_2$ (Figure 6B). The nonlinear increase of O$_2$ production with Fe(OH)$_{3(s)}$ dosage is likely due to the limitation on the available Fe(III) reactive surface sites, e.g.,
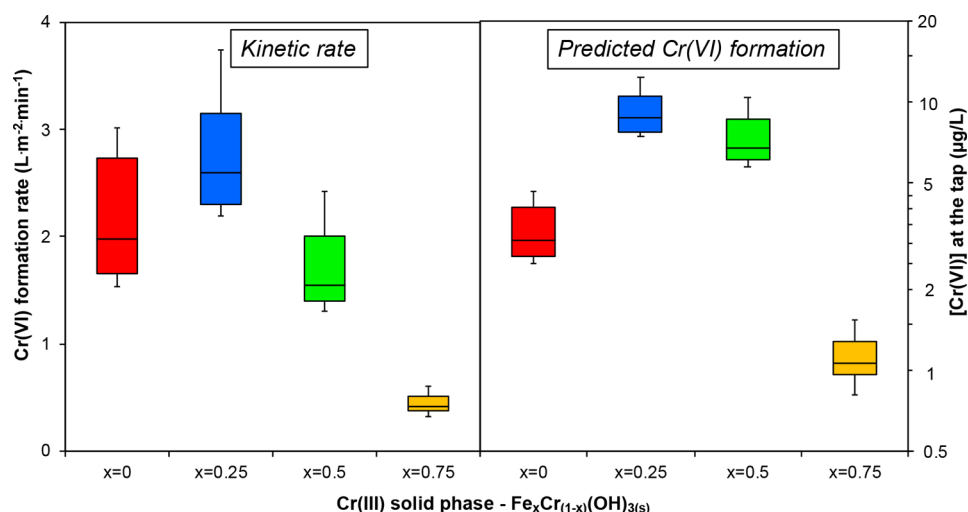
Figure 7. Box-plot of predicted Cr(VI) formation rate constants and the enhanced Cr(VI) formation in drinking-water distribution systems. The solid line in each box is the median value; the lower and upper box edges are the 25th and 75th percentiles, respectively. Whisker bars represent the 5th and 95th percentiles. The percentile distributions are predicted on the basis of Cr(VI) formation rate constants obtained from this study and statistical distributions of bromide concentration in U.S. source waters. The data with pure phase Cr(III) solids where $x = 0$ was obtained from a prior study.[12] The kinetics model simulation on enhanced Cr(VI) formation is based on a water distribution system with 0.3 mg/L chlorine residual, 100 μg/L residual Cr(III) solids, and a residence time of 2 days.

aggregation of ferrihydrite particles during the course of the reaction. A correlation between oxygen generation and chlorine decay in the presence of ferrihydrite exhibited a stoichiometric ratio of 0.1 (SI Figure S7), suggesting that the decay of chlorine was enhanced by Fe(III) surface sites with $Fe_xCr_{(1-x)}(OH)_{3(s)}$. Similar halogen oxidant decay (e.g., HOCl and ClO_2) enhanced by transition metal oxides has been previously observed.[49−51]

Accordingly, the reaction stoichiometry of $\Delta Cr(VI)/\Delta HOCl$ during $Fe_xCr_{(1-x)}(OH)_{3(s)}$ oxidation by chlorine was further adjusted to consider the pathway of Fe(III)-induced chlorine decay and O_2 generation. An oxygen coefficient α was introduced to quantify the contribution of reactions that decomposed chlorine to generate O_2 while not converting Cr(III) to Cr(VI) in $Fe_xCr_{(1-x)}(OH)_{3(s)}$. The value of α represented the extent of chlorine scavenging reactions without generating Cr(VI), i.e., two reaction pathways that generate O_2: Cr(V) intermediate formation and Fe(III)-induced chlorine decay. When all reaction mechanisms were considered, the adjusted stoichiometry of $\Delta[Cr(VI)]/(\Delta HOCl - \alpha \times \Delta O_2)$ approached the expected value of 0.67 (orange-color box plots in Figure 4).

Overall, the value of α ranged between 2 and 7, but increased with the number of x in $Fe_xCr_{(1-x)}(OH)_{3(s)}$ (SI Figure S8). A larger α coefficient indicates a stronger inhibitive effect on Cr(VI) formation via $Fe_xCr_{(1-x)}(OH)_{3(s)}$ oxidation by chlorine. The positive correlation between α and x represents an increasing importance of the Fe(III)-induced chlorine decay pathway as the Fe(III) molar fraction increases in $Fe_xCr_{(1-x)}(OH)_{3(s)}$.

As chlorine is decayed into dissolved O_2 and chloride by Fe(III) surface sites on $Fe_xCr_{(1-x)}(OH)_{3(s)}$, it can also involve the generation of short-lived intermediate radicals including hydroxyl radical (HO$^\bullet$), chlorine atom (Cl$^\bullet$) and chlorine dimer $Cl_2^{\bullet-}$ prior to the formation of chloride and O_2.[52,53] Possible reactions were discussed in SI Text S2. To further evaluate the generation of reactive radical species, experiments were conducted with the addition of excess benzoic acid (BA)

as a scavenger for all reactive radicals. BA reacts quickly with HO$^\bullet$, Cl$^\bullet$ and $Cl_2^{\bullet-}$, but does not react with chlorine or interfere with chlorine decay in the presence of Fe(III) and Cr(III) solids (SI Figure S9). Results showed that in the presence of BA, the formation of O_2 via chlorine decay by $Fe(OH)_{3(s)}$ was completely inhibited (SI Figure S10A). The amount of O_2 generation via chlorine decay by $Fe_xCr_{(1-x)}(OH)_{3(s)}$ also decreased by approximately 40% in the presence of BA (SI Figure S10B). This observation suggests that about 40% of oxygen formation was contributed by Fe(III) sites on $Fe_xCr_{(1-x)}(OH)_{3(s)}$ that involves the formation of reactive radical species, with the remaining 60% contributed by Cr(III) sites via the Cr(V) intermediate formation/decay.

Environmental Implications. Drinking water distribution systems are reactive and lined with corrosion scales that are in situ sources of trace metal contaminants including chromium. In iron-containing distribution systems, accumulated Cr(III) in corrosion scales was reactive with residual chlorine, but the existence of Fe(III) in corrosion scales can greatly diminish Cr(VI) formation. For example, based on the Cr(VI) formation rate constants obtained from this study at different levels of pH, bicarbonate and bromide, as well as the statistical distribution of bromide concentrations in U.S. source waters,[54] a kinetics model was established (SI Text S3). The model predicts that the 50th percentile Cr(VI) concentration in tap water can increase substantially between 1 and 9 μg/L, and a higher molar fraction of Fe(III) in the $Fe_xCr_{(1-x)}(OH)_{3(s)}$ solid phase generally leads to a lower Cr(VI) formation potential (Figure 7).

To control Cr(VI) level at the tap, especially for aging drinking water distribution infrastructure composed of corroded iron piping materials and free chlorine as the residual disinfectant, effective water management strategies include pH adjustment and bicarbonate control as post-treatment steps prior to entrance to drinking water distribution systems, and the prevention of halide input in source water, for example, seawater intrusion or point source

discharge from energy sector. A mobilization or resuspension of Cr(III)-containing iron oxide will increase the risk of in situ Cr(III) conversion to Cr(VI) in drinking water distribution system. Considering that a majority of drinking water distribution infrastructure is based on iron material dominant pipe system, a better control of the redox reactivity of iron-containing Cr(III) solids is important to develop future water management strategies.

■ ASSOCIATED CONTENT

Ⓢ Supporting Information

The Supporting Information is available free of charge on the ACS Publications website at DOI: 10.1021/acs.est.7b06013.

> Additional descriptions on figures of zeta potential of Cr(III)−Fe(III) hydroxides, Cr(III) solid oxidation kinetics and standard redox potential calculations (PDF)

■ AUTHOR INFORMATION

Corresponding Author

*Phone (951) 827-2076; fax (951) 827-5696; e-mail: haizhou@engr.ucr.edu.

ORCID Ⓘ

Haizhou Liu: 0000-0003-4194-2566

Notes

The authors declare no competing financial interest.

■ ACKNOWLEDGMENTS

■ REFERENCES

(1) Vincent, J. *The Nutritional Biochemistry of Chromium(III)*; Elsevier, 2011.

(2) Nriagu, J. O.; Nieboer, E. *Chromium in the Natural and Human Environments*; John Wiley & Sons, 1988.

(3) California Environmental Protection Agency; State Water Resources Board. Hexavalent Chromium in Drinking Water. http://www.waterboards.ca.gov/drinking_water/certlic/drinkingwater/Chromium6.shtml.

(4) United States Environmental Protection Agency. Unregulated Contaminant Monitoring Rule 3 (UCMR 3).http://water.epa.gov/lawsregs/rulesregs/sdwa/ucmr/ucmr3/index.cfm.

(5) Loock-Hattingh, M. M.; Beukes, J. P.; van Zyl, P. G.; Tiedt, L. R. Cr(VI) and conductivity as indicators of surface water pollution from ferrochrome production in South Africa: four case studies. *Metall. Mater. Trans. B* **2015**, *46*, 2315−2325.

(6) du Preez, S. P.; Beukes, J. P.; van Zyl, P. G. Cr(VI) generation during flaring of CO-Rich off-gas from closed ferrochromium submerged arc furnaces. *Metall. Mater. Trans B* **2015**, *46*, 1002−1010.

(7) Kotaś, J.; Stasicka, Z. Chromium occurrence in the environment and methods of its speciation. *Environ. Pollut.* **2000**, *107* (3), 263−283.

(8) Jardine, P. M.; Mehlhorn, T. L.; Bailey, W. B.; Brooks, S. C.; Fendorf, S.; Gentry, R. W.; Phelps, T. J.; Saiers, J. E. Geochemical processes governing the fate and transport of chromium(III) and chromium (VI) in soils. *Vadose Zone J.* **2011**, *10*, 1058−1070.

(9) Oze, C.; Bird, D. K.; Fendorf, S. Genesis of hexavalent chromium from natural sources in soil and groundwater. *Proc. Natl. Acad. Sci. U. S. A.* **2007**, *104*, 6544−6549.

(10) Gonzalez, A. R.; Ndung'u, K.; Flegal, A. R. Natural occurrence of hexavalent chromium in the Aromas Red Sands Aquifer, California. *Environ. Sci. Technol.* **2005**, *39*, 5505−5511.

(11) Chebeir, M.; Chen, G.; Liu, H. Emerging investigators series: frontier review: occurrence and speciation of chromium in drinking water distribution systems. *Environ. Sci.: Water Res. Technol.* **2016**, *2* (6), 906−914.

(12) Chebeir, M.; Liu, H. Kinetics and mechanisms of Cr(VI) formation via the oxidation of Cr(III) solid phases by chlorine in drinking water. *Environ. Sci. Technol.* **2016**, *50* (2), 701−710.

(13) Peng, C.-Y.; Korshin, G. V.; Valentine, R. L.; Hill, A. S.; Friedman, M. J.; Reiber, S. H. Characterization of elemental and structural composition of corrosion scales and deposits formed in drinking water distribution systems. *Water Res.* **2010**, *44* (15), 4570−4580.

(14) Peng, C.-Y.; Korshin, G. V. Speciation of trace inorganic contaminants in corrosion scales and deposits formed in drinking water distribution systems. *Water Res.* **2011**, *45* (17), 5553−5563.

(15) Peng, C.-Y.; Ferguson, J. F.; Korshin, G. V. Effects of chloride, sulfate and natural organic matter (NOM) on the accumulation and release of trace-level inorganic contaminants from corroding iron. *Water Res.* **2013**, *47* (14), 5257−5269.

(16) Friedman, M. *Metals Accumulation and Release within the Distribution System: Evaluation and Mitigation*; Park City Municipal Corporation (Utah); Water Research Foundation: Denver, CO, 2016.

(17) Frey, M.; Seidel, C.; Edwards, M. *Occurrence Survey of Boron and Hexavalent Chromium*; American Water Works Association: Denver, CO, 2005.

(18) Liu, J.; Chen, H.; Yao, L.; Wei, Z.; Lou, L.; Shan, Y.; Endalkachew, S.; Mallikarjuna, N.; Hu, B.; Zhou, X. The spatial distribution of pollutants in pipe-scale of large-diameter pipelines in a drinking water distribution system. *J. Hazard. Mater.* **2016**, *317*, 27−35.

(19) Cui, Y.; Liu, S.; Smith, K.; Yu, K.; Hu, H.; Jiang, W.; Li, Y. Characterization of corrosion scale formed on stainless steel delivery pipe for reclaimed water treatment. *Water Res.* **2016**, *88*, 816−825.

(20) Hill, A. S.; Friedman, M. J.; Reiber, S. H.; Korshin, G. V.; Valentine, R. L. Behavior of trace inorganic contaminants in drinking water distribution systems. *J. - Am. Water Works Assoc.* **2010**, *102* (7), 107−118.

(21) Melendres, C. A.; Pankuch, M.; Li, Y. S.; Knight, R. L. Surface enhanced Raman spectroelectrochemical studies of the corrosion films on iron and chromium in aqueous solution environments. *Electrochim. Acta* **1992**, *37* (15), 2747−2754.

(22) Guo, Q. Increase of lead and chromium in drinking water from using cement-motar-lined pipes: initial modeling and assessment. *J. Hazard. Mater.* **1997**, *56*, 181−213.

(23) Gonzalez, S.; Lopez-Roldan, R.; Cortina, J. Presence of metals in drinking water distribution networks due to pipe material leaching: a review. *Toxicol. Environ. Chem.* **2013**, *95* (6), 870−889.

(24) Papassiopi, N.; Vaxevanidou, K.; Christou, C.; Karagianni, E.; Antipas, G. S. E. Synthesis, characterization and stability of Cr(III) and Fe(III) hydroxides. *J. Hazard. Mater.* **2014**, *264*, 490−497.

(25) Eary, L. E.; Rai, D. Kinetics of chromate reduction by ferrous iron. *Environ. Sci. Technol.* **1996**, *30* (5), 1614−1617.

(26) Dai, C.; Zuo, X.; Cao, B.; Hu, Y. Homogeneous and heterogeneous (Fe$_x$Cr$_{1-x}$)(OH)$_3$ precipitation: implications for Cr sequestration. *Environ. Sci. Technol.* **2016**, *50* (4), 1741−1749.

(27) Pan, C.; Catalano, J. G.; Qian, A.; Giammar, D. E. Rates of Cr(VI) generation from Cr$_x$Fe$_{1-x}$(OH)$_3$ solids upon reaction with manganese oxide. *Environ. Sci. Technol.* **2017**, *51* (21), 12416−12423.

(28) Oze, C.; Bird, D. K.; Fendorf, S. Genesis of hexavalent chromium from natural sources in soil and groundwater. *Proc. Natl. Acad. Sci. U. S. A.* **2007**, *104* (16), 6544−6549.

(29) Hausladen, D. M.; Fendorf, S. Hexavalent chromium generation within naturally structured soils and sediments. *Environ. Sci. Technol.* **2017**, *51* (4), 2058–2067.

(30) McNeill, L.; McLean, J.; Edwards, M.; Parks, J. State of the science of hexavalent chromium in drinking water; *Water Res. Found.*, **2012**.

(31) Lindsay, D. R.; Farley, K. J.; Carbonaro, R. F. Oxidation of Cr[III] to Cr[VI] during chlorination of drinking water. *J. Environ. Monit.* **2012**, *14* (7), 1789.

(32) Lai, H.; McNeill, L. S. Chromium redox chemistry in drinking water systems. *J. Environ. Eng.* **2006**, *132* (8), 842–851.

(33) Schock, M. R.; Wagner, I.; Oliphant, R. J. *Internal Corrosion of Water Distribution Systems*; American Water Works Association: Denver, CO, 1996.

(34) Liu, H.; Schonberger, K. D.; Korshin, G. V.; Ferguson, J. F.; Meyerhofer, P.; Desormeaux, E.; Luckenbach, H. Effects of blending of desalinated water with treated surface drinking water on copper and lead release. *Water Res.* **2010**, *44* (14), 4057–4066.

(35) Li, W.; Orozco, R.; Camargos, N.; Liu, H. Mechanisms on the impacts of alkalinity, pH, and chloride on persulfate-based ground-water remediation. *Environ. Sci. Technol.* **2017**, *51* (7), 3948–3959.

(36) Allard, S.; Fouche, L.; Dick, J.; Heitz, A.; von Gunten, U. Oxidation of manganese(II) during chlorination: role of bromide. *Environ. Sci. Technol.* **2013**, *47* (15), 8716–8723.

(37) Good, K. D.; VanBriesen, J. M. Power plant bromide discharges and downstream drinking water systems in Pennsylvania. *Environ. Sci. Technol.* **2017**, *51* (20), 11829–11838.

(38) Hansel, C. M.; Wielinga, B. W.; Fendorf, S. Structural and compositional evolution of Cr/Fe solids after indirect chromate reduction by dissimilatory iron-reducing bacteria. *Geochim. Cosmo-chim. Acta* **2003**, *67* (3), 401–412.

(39) Jambor, J. L.; Dutrizac, J. E. Occurrence and Constitution of natural and synthetic ferrihydrite, a widespread iron oxyhydroxide. *Chem. Rev.* **1998**, *98* (7), 2549–2586.

(40) Rice, E. W.; Bridgewater, L. *Standard Methods for the Examination of Water and Wastewater*; American Public Health Association: Washington, D.C., 2012.

(41) Génin, J.-M. R.; Dhouibi, L.; Refait, P.; Abdelmoula, M.; Triki, E. Influence of phosphate on corrosion products of iron in chloride-polluted-concrete-simulating solutions: ferrihydrite vs green rust. *Corrosion* **2002**, *58* (6), 467–478.

(42) Benali, O.; Abdelmoula, M.; Refait, P.; Génin, J.-M. R. Effect of orthophosphate on the oxidation products of Fe(II)-Fe(III) hydroxycarbonate: the transformation of green rust to ferrihydrite. *Geochim. Cosmochim. Acta* **2001**, *65* (11), 1715–1726.

(43) Kumar, K.; Margerum, D. W. Kinetics and mechanism of general acid-assisted oxidation of bromide by hypochlorite and hypochlorous acid. *Inorg. Chem.* **1987**, *26* (16), 2706–2711.

(44) Westerhoff, P.; Chao, P.; Mash, H. Reactivity of natural organic matter with aqueous chlorine and bromine. *Water Res.* **2004**, *38* (6), 1502–1513.

(45) Echigo, S.; Minear, R. A. Kinetics of the reaction of hypobromous acid and organic matters in water treatment processes. *Water Sci. Technol.* **2006**, *53* (11), 235–243.

(46) Richard, F. C.; Bourg, A. C. M. Aqueous geochemistry of chromium: A review. *Water Res.* **1991**, *25* (7), 807–816.

(47) Gómez, V.; Callao, M. P. Chromium determination and speciation since 2000. *TrAC, Trends Anal. Chem.* **2006**, *25* (10), 1006–1015.

(48) Benjamin, M. M.; Lawler, D. F. *Water Quality Engineering: Physical/Chemical Treatment Processes. Chapter 10: Redox Processes and Disinfection*; John Wiley & Sons, Inc.: Hoboken, NJ, 2013.

(49) Liu, C.; von Gunten, U.; Croué, J.-P. Enhanced chlorine dioxide Decay decay in the presence of metal Oxides: Relevance to drinking water distribution systems. *Environ. Sci. Technol.* **2013**, *47* (15), 8365–8372.

(50) Lister, M. W. Decomposition of sodium hypochlorite: the catalyzed reaction. *Can. J. Chem.* **1956**, *34* (4), 479–488.

(51) Sandin, S.; Karlsson, R. K. B.; Cornell, A. Catalyzed and uncatalyzed decomposition of hypochlorite in dilute solutions. *Ind. Eng. Chem. Res.* **1956**, *34* (4), 479–488; *Ind. Eng. Chem. Res.* **2015**, *54* (15), 3767–3774.

(52) Kornweitz, H.; Burg, A.; Meyerstein, D. Plausible mechanisms of the Fenton-like reactions, M = Fe(II) and Co(II), in the presence of RCO2(−) substrates: are OH(●) radicals formed in the process? *J. Phys. Chem. A* **2015**, *119* (18), 4200–4206.

(53) Heckert, E. G.; Seal, S.; Self, W. T. Fenton-like reaction catalyzed by the rare earth inner transition metal cerium. *Environ. Sci. Technol.* **2008**, *42* (13), 5014–5019.

(54) Wilson, J. M.; Wang, Y.; VanBriesen, J. M. Sources of high total dissolved solids to drinking water supply in Southwestern Pennsylvania. *J. Environ. Eng.* **2013**, *140*, B4014003.